②

OFFICE OF NAVAL RESEARCH

GRANT or CONTRACT N00014-77-C-1234

R & T Code 413 h 012

Technical Report No. 4

UPS, XPS, AND HREELS Characterization of Trimethyl Indium Adsorbed on Si(110)*

by

Yue Bu, Jason S. Chu, David W. Shinn, and M. C. Lin

Prepared for Publication
in
The Chemistry of Materials

UPS, XPS, AND HREELS Characterization of Trimethyl Indium Adsorbed on Si(110)*

Yue Bu, Jason S. Chu, David W. Shinn, and M. C. Lin*
Chemistry Department
Emory University
Atlanta, Georgia 30322

ABSTRACT

The techniques of UPS, XPS, HREELS, and REMPI are utilized to investigate the thermal decomposition of Trimethylindium (TMIn) on Si substrates under various surface coverage conditions. In the 140-1100 K temperature range, three regions of varying characteristics are found. Firstly, below 630 K, TMIn adsorbs molecularly with little further reaction on the substrate. In the 630-890 K region, the decomposition of adsorbed TMIn appears to take place. The presence of CH_x(ad) ($x \leq 3$), Si-H, and Si-C species on the surface are confirmed by UPS and/or HREELS. XPS shows a steady shift to lower binding energies for the C1s photoelectrons and UPS shows a see-saw-like shifting for the In 4d photoelectrons, first to lower then to higher binding energies. Furthermore, REMPI/MS measurements provide evidence for the steady-state desorption of CH_3 radicals in this thermal region. Above 890 K, it appears that a thermally more complex process persists whereby In desorbs and C is deposited onto the surface.

* Work supported by the Office of Naval Research.

INTRODUCTION

In the past decade, organometallic chemical vapor deposition (OMCVD) of III-V compound semiconductors has experienced explosive growth; one such system having applications in optoelectronic and microwave devices is InP (1). From a practical point of view, numerous devices have been fabricated and reported to have device-quality operating parameters; on the other hand, little is known about the actual reaction mechanisms controlling the deposition process. It is perceived that such information would benefit the further development of OMCVD and, therefore, we have initiated an investigation of the thermal decomposition dynamics of trimethylindium (TMIn), a common organometallic precursor in InP OMCVD, on Si(110) substrates.

While a number of studies have been undertaken regarding the homogeneous gas-phase decomposition of TMIn (2-9), surprisingly little is known concerning the behavior of TMIn on heated Si surfaces. However, a fair amount of literature has been produced regarding similar studies on relatives of TMIn, i.e., trimethylaluminum (TMAl)(10,11) and trimethylgallium (TMGa) (12,13). Although gas-phase TMAl is predominantly present in the dimer form at room temperature(14) and TMIn and TMGa are monomers(15) under such conditions, a number of similar diagnostics accompanying the decomposition of TMAl or TMGa on heated Si surfaces may also be expected for TMIn.

The adsorption and thermal decomposition of TMAl and TMGa have been investigated by Masel and coworkers (11,13) under submonolayer conditions. Utilizing the techniques of temperature-programmed desorption (TPD), X-ray photoelectron spectroscopy (XPS), and high resolution electron energy loss spectroscopy (HREELS), they were able to elucidate the mechanism of the decomposition of TMAl or TMGa on sequentially heated Si substrates. Furthermore, it was also shown that C incorporation within the deposited material was an intrinsic part of the decomposition process.

In the present study, we have examined TMIn adsorption and decomposition on Si(110) substrates using ultraviolet photoelectron spectroscopy (UPS), XPS, HREELS, and briefly, resonance-enhanced multiphoton ionization (REMPI) for the detection of CH_3 radicals, whose desorption was first reported by Squire et al. (10,12) under steady-state deposition conditions.

EXPERIMENTAL

The experiments were carried out in a custom-made UHV system (Leybold, Inc.) schematically shown in Figure 1. The system is composed of two chambers, one for deposition and the other for surface analysis, separated by a specially designed metal compression seal. Samples can be positioned as well as transferred between sample rods through two independent drive systems and a magnetically operated sample transfer arm.

The deposition chamber is equipped with an Ar^+ ion gun for surface bombardment and a differentially pumped quadrupole mass spectrometer (QMS)(Extrel Corp., Model C-50) mounted vertically above the surface region for gas phase analysis during deposition. A 2-mm skimmer assembly separates the deposition chamber from the QMS analysis region with base pressures of 1×10^{-9} Torr and 2×10^{-10} Torr, respectively, each achieved via pumping by 360 L/s turbomolecular pumps (TMP)(Leybold-Heraus, Inc.). The QMS ionization region can also be probed through sapphire windows for radical detection by REMPI.

The larger surface analysis chamber is further separated into two main regions. One region is equipped with Auger electron spectroscopy (AES), XPS (Al $K\alpha_{1,2}$ at 1486.6 eV), and UPS (He II at 40.8 eV), all utilizing a 180° hemispherical electrostatic condenser analyzer for charged particle detection. The second region, mu-metal shielded except for two 10-cm holes allowing for the sample drive system, is equipped with HREELS. The chamber is pumped to a base pressure of 4×10^{-11} Torr through the use of a TMP, liquid nitrogen cold trap, titanium sublimation pump, and an ion pump.

Si(110) single crystal surfaces were cut from 2" wafers (10 ohm-cm, P-doped, Virginia Semiconductor) into 1.5 x 1.0 cm^2 samples. After boiling in dilute HF and ultrasonicating in distilled-deionized H_2O, the samples were suspended between two Ta clips and repeatedly subjected to Ar^+ bombardment and flashing until no C, O, or other impurities could be detected by AES and/or XPS. Resistive heating was accomplished by utilizing a standard DC power supply (Hewlett Packard, Model 6012B). Above 925 K, a two-color pyrometer (Capintec, "Hot Shot") was used for temperature measurements; below 925 K, temperatures were estimated by measuring the sample resistance and extrapolating from the higher temperature/resistance calibration curves for each individual sample. For comparison, a Chromel-Alumel (Omega Corp.) thermocouple feedthrough assembly could also be utilized for temperature estimation.

TMIn was prepared by diluting the electronic grade source (Morton Co.) with UHP grade Ar gas (Specialty Gases Southeast) on a separate glass vacuum system. The sample mixture was then introduced into the deposition chamber through a 1-mm I.D. stainless steel tube located approximately 7 mm away and about 45 degrees off-normal from the surface ensuring that the effusive beam was directed towards the surface. The gas flow rate was adjusted with a metering valve (Nupro).

During the experiments, a clean surface at 300 K, unless otherwise stated, was dosed with an indicated amount of TMIn, after which UPS, XPS, and/or HREELS spectra were recorded. Generally, a 300 K dosed sample was sequentially annealed to higher temperatures and then cooled to 300 K in order to record successive spectra.

CH_3 radical production was observed under steady state dosing conditions at various temperatures via REMPI at 333.5 nm (Exciton, Inc., P-terphenyl) with the use of an excimer pumped dye laser system (Lambda Physik).

RESULTS AND DISCUSSION

UPS

The series of UPS spectra shown in Figure 2 illustrate the effects of sequential annealing on a TMIn dosed (0.5 Langmuir(L)) Si(110) substrate.

When dosed at 300 K, the density of Si surface states centered at 39.3 eV and 39.9 eV decreased significantly; also, the Si surface state structure near 35.2 eV was almost obscured completely. In the mean time, new bands appeared at 23.8 eV and 24.7 eV (In $4d_{3/2,5/2}$)(16) , 26.0 eV (C 2s (17) believed to be associated with -CH_3), 33.9 eV (superimposed 1e", 3a', and 2e' $\sigma_{C\text{-}H}$ molecular orbitals (MO) of TMIn(ad))(18), and 36.9 eV (3e' MO of TMIn(ad) most likely associated with metal-carbon bonding)(18). These effects are mostly due to the predominant molecular adsorption of TMIn(ad).

Although the In 4d data compares favorably to that of bulk or surface-related In (16), it should be pointed out that the TMIn(ad) MO and In 4d assignments above are 5-7 eV lower in binding energy than those obtained from gas phase UPS analyses of TMIn (18,19). Aside from a relatively small shift due to the different chemical environments, most of this difference is due to the inherent presence of a significant spectrometer/surface work function (ca. 4.6eV) in our work. Additionally, the In 4d signals are shifted more (ca. 7 eV) than the signals arising from the MOs of TMIn (ca. 5-6 eV). This suggests that initially the central In atom may be more tightly bound to the surface than the surrounding $-CH_3$ groups which, in turn, could induce a distortion in the planer structure of TMIn.

Upon annealing to higher temperatures, a number of observations were noted. Firstly, the Si surface states continued to decrease and broaden into one large band centered at slightly higher binding energies. This is probably a result of differential surface state bonding to various species produced by the progressive surface cracking of TMIn(ad)(e.g., $-CH_x$ ($x \leq 3$), -H, -C, as well as In and/or In-containing radicals). In support of this argument, the C 2s band at 26.0 eV related to $-CH_3$ and the TMIn(ad) MO band structures at 33.8 eV and 36.9 eV progressively decreased and disappeared at about 890 K while two new bands on the higher binding energy side of the broadened $\sigma_{C\text{-}H}$ band system emerged at around 760 K and increased in intensity as the temperature rose. This structure, due to $-CH_2$ (17) and probably -CH species as well, disappeared at 975 K and above. Meanwhile, from 300 K to near 710 K, the In 4d structure shifted to higher K.E.s; from approximately 710 K to 840 K, these lines inversely shifted to K.E.s even lower than those observed for the 300 K dosed sample.

The above see-saw-like surface-induced shift in the In $4d_{3/2,5/2}$ structure, although not totally unexpected, appears to be in opposite directions to that determined from high resolution UPS spectra taken on gas-phase TMIn.

Bancroft et al. (19) assigned higher binding energy 4d structure to the In(CH_3)$_2$ radical and lower binding energy structure to molecular TMIn. Though not observed, they calculated the atomic In structure to be still lower in binding energy. In our work here, it is reasonable to conclude that the structure upon adsorption is primarily due to molecularly adsorbed TMIn. However, as the temperature is raised to the point where In-C bonds are beginning to break, the structure shifts to lower binding energies before shifting back to higher binding energies at yet higher temperatures where most In-C bonds are believed to have been broken and, more than likely, replaced by In-Si bonds. At present, there is not a clear explanation for the temperature dependence on the directional character of this binding energy inversion for the In 4d levels. Nevertheless, it would be reasonable to suspect that the In 4d orbitals initially become less bound to the surface as In-C bonds are replaced by In-Si bonds whereas at higher temperatures In(ad) may be diffusing to more highly bound surface or sub-surface sites resulting in the observed inversion. Such high temperature surface diffusion phenomena are well known for metals such as Al or Ag on Si(111) surfaces. For temperatures of 975 K and above, no In 4d structure was evident indicating complete In desorption. After flashing at 1470 K, a clean surface was re-established.

XPS

Figure 3 shows a series of C_{1s} XPS spectra taken under the same conditions as those in Figure 2 except that 5 L TMIn instead of 0.5 L was dosed on a Si(110) surface. Between 300 K and 620 K a single peak centered at 1199.8 eV was observed with little noticeable changes due to sequential annealing. At 670 K, there was an obvious attenuation and shifting of the peak towards higher K.E.s. There were no other distinct changes until 760 K, above which there was further shifting to even higher K.E.s; no significant signal attenuation was noted up to 990 K. It should be noted that experiments carried out with 0.8 L dosage produced essentially the same results.

Except for the fact that no absolute calibrations of work function effects have been performed to position the surface C 1s XPS line to its accepted value, these results are in agreement with those presented by Gow et al. (11) and Lee et al.(13) for similar XPS studies performed on the decomposition of TMAl or TMGa, respectively, on Si(100) substrates. Briefly, sequential annealing of a TMIn dosed Si(110) substrate leads to the incorporation of measurable quantities of chemisorbed C. In fact, C remains on the surface at temperatures greater than those required to desorb essentially all of the In species.

Additionally, In $3d_{3/2,5/2}$ XPS spectra in the 1028-1048 eV range, obtained under identical conditions as for the C 1s XPS spectra above, exhibited similar yet less dramatic changes than the UPS results described above for the $4d_{3/2,5/2}$ spectra.

Shown in Figure 4 are In $3d_{3/2,5/2}$ XPS spectra obtained in a somewhat more practical manner than the other data presented within this report. After flashing a sample to near 1470 K, background spectra were recorded. Then, the Si surface was exposed to a 150 L dose of TMIn at a particular temperature, after which another series of spectra were recorded. Finally, the dosed surface was annealed at 1000 K and a third set of spectra were taken, providing the post-annealed data. The pre-annealed and post-annealed series of spectra were generated by subtracting the corresponding background spectra from the dosed spectra and the dosed/annealed spectra, respectively.

Below a dosing temperature of ca. 650 K all the pre-annealed dosings produced similar In 3d spectral differences. Following the annealing treatment, In 3d signals essentially disappeared. For samples dosed at ca. 750 K, significantly smaller In 3d signals having slightly higher K.E.s resulted with little noticeable desorption effected by the annealing treatment; higher dosing temperatures produced very similar results.

These preliminary results are stimulating. Firstly, the data suggest that TMIn and/or partially fragmented relatives predominantly adsorb in a weakly bound manner at temperatures below ca. 750 K and are desorbed upon quickly annealing the dosed surface to 1000 K. At temperatures of ca. 750 and above, although less In and/or In containing species reach and/or remain on the surface as evidenced by the reduced signals, those which do apparently bind more tightly to the surface as compared to TMIn dosing at lower temperatures and subsequently annealed to higher temperatures (see UPS and HREELS results). Additional studies are presently underway to fully understand the effects of high temperature dosing as well as post annealing at higher temperatures. It will also be of interest to monitor C 1s signals in order to substantiate preliminary findings that the In/C ratio on the surface may be enhanced in the 700-800 K range. It is interesting to point out that this is near the 770-900 K temperatures which have been used in a number of InP CVD processing schemes (1).

HREELS

Figure 5 shows a series of HREELS spectra obtained under similar conditions as described for Figure 2. After dosing at 140 K, there were broad bands at 90 meV, 182 meV, and 377 MeV with a shoulder at 148 meV, corresponding to ρ-CH_3, δ-CH_3, υ-CH_3 and δ-CH_3 (11,13,20) vibrations, respectively. After warming to 280 K, all of the main bands were attenuated by

2-4 times while the shoulder became much less distinguished. Except for a small amount of peak attenuation as well as nominal shifts in energy, the structure remained unchanged after annealing to temperatures lower than 640 K. At about 640 K, a new band at 263 meV due to Si-H vibration (21) began to emerge and continued to increase until it started to decrease at temperatures higher than 800 K. Meanwhile, the band intensities near 182 meV and 377 meV continuously decreased with slight shifts to lower energies in this thermal region with the 182 meV band essentially absent above 800 K. Finally, as the temperature was progressively raised to 1180 K, the 90 meV band appeared to decrease while a new band developed at 110 meV; this energy loss correlates well with that expected for a Si-C stretch (21).

The above HREELS results are in fair agreement with those of Gow et al. (11) and Lee et ai. (13) for the decomposition of TMAl and TMGa, respectively, on Si (100) substrates.

OTHER MEASUREMENTS

2 + 1 REMPI/MS signals at 333.5 nm and 15 amu substantiated the production of CH_3 radicals during the steady-state thermal decomposition of TMIn on Si(110). This observation is in qualitative agreement with Squire et al. (10,12) whereby $-CH_3$ radicals were also observed during the steady-state thermal decomposition of TMAl or TMGa on various heated surfaces. Quantitative studies are presently underway to further delineate the kinetic parameters for this process.

Electron ionization (EI)/MS measurements under similar conditions also showed CH_3, CH_4, and $In(CH_3)_x$ (x=0, 1,2) signals with CH_3 and $In(CH_3)_2$ being the major species. TPD studies will be undertaken shortly.

CONCLUSIONS

In view of the above results and discussion, we conclude that the mechanisms controlling the adsorption and subsequent thermal decomposition of TMIn on heated Si(110), are quite diverse and complex. Firstly, with dosing at low temperatures followed by further annealing at higher temperatures, we believe that TMIn initially adsorbs via a distortion in its planer structure with the central In atom bonding closely to the Si substrate. This is supported by the TMIn(ad) UPS results. HREELS results unequivocally provide evidence for the formation of Si-H species on the surface at the intermediate temperatures of 600-800 K. For this to occur, $-CH_2$ type species must also be present. Furthermore, the XPS and HREELS experiments confirmed the presence of surface C at higher temperatures and, thus, a "trickling" down from $-CH_3$ type species must also occur. This $-CH_2$ type species to -C type species propagation is somewhat elusively justified in the form of notable energy-shifts in approximately the same thermal ranges for the various -C or $-CH_x$ related spectral bands observed using UPS, XPS, and HREELS. The decisive characterization of the numerous pathways for this progression is beyond the scope of the present investigation.

The observed UPS, XPS, HREELS, and REMPI results, however, may be qualitatively summarized as follows:

at Ts < 630 K:

$$(CH_3)_3\,In\ (g) \rightarrow (CH_3)_3\,In\ (a)$$

at 630 K < Ts < 890 K:

$$(CH_3)_3\,In\ (a) \rightarrow x\ CH_3\ (a) + (CH_3)_{3-x}\,In\ (a)$$

$$CH_3\ (a) \rightarrow y\ H\ (a) + CH_{3-y}\ (a)$$

$$CH_3\ (a) \rightarrow CH_3\ (g)$$

at Ts > 890 K:

$$In\ (a) \rightarrow In\ (g)$$

where

$x, y = 1\text{-}3.$

ACKNOWLEDGEMENTS

The authors would like to acknowledge Mr. Bill Day for his expert help in computer-instrument interfacing. Support of this work by the Office of Naval Research (Contract No.N00014-89-J-1235) and the Emory University research funds is gratefully acknowledged.

REFERENCES:

1. Razeghi, M. *Semiconductors and Semimetals* (1990) **31,** 243.

2. Karlicek, R., Long, J. A., Donnelly, V. M. *J. Crystal Growth* (1984) **68,** 123.

3. Haigh, J.; O'Brien, S. *J. Crystal Growth* (1984) **68,** 550.

4. Larsen, C. A., Stringfellow, G. B. *J. Crystal Growth* (1986) **75,** 247.

5. Jackson, D. A. Jr., *J. Crystal Growth* (1988) **87,** 212.

6. Buchan, N. I., Larsen, C. A., Stringfellow, G. B. *Appl. Phys. Lett.* (1987) **51,** 1024.

7. Buchan, N. I., Larsen, C. A., Stringfellow, G. B. *J.Crystal Growth* (1988) **92,** 591.

8. Hebner, G. A., Killeen, K. P., Biefeld, R. M. *J. Crystal Growth* (1989) **98,** 293.

9. Larsen, C. A., Buchan, N. I. , Li, S. H., Stringfellow, G. B. *J. Crystal Growth* (1990) **102,** 103.

10. Squire, D. W., Dulcey, C. S., Lin, M. C. J. Voc. Sci. Technol, B, (1985) 3, 1513.

11. Gow, T. R., Lin, R., Cadwell, L. A. Lee, F., Backman, A. L., Masel, R. I. *Chem. Mater.* (1989) **1,** 406.

12. Squire, D. W., Dulcey, C. S., Lin, M. C. *Mater. Res. Soc. Symp. Proc.* (1988) **101,** 301.

13. Lee, F., Backman, A. L., Lin, R., Gow T. R., Masel, R. I. *Surf. Sci.* (1989) **216,** 173-188.

14. Kvisle S., Ritter, E. *Spectrochim. Acta* (1984) **40,** 939.

15. (a) Kraus, C. A., Toonder, F. E., *Proc. Nat. Acad.Sci.* (1933) **19,** 292. (b) Laubengayer, A. W., Gilliam, W. F., *J. Am. Chem. Soc.* (1941) **63,** 477.

16. Vitomirov, I. M., Aldao, C. M., Lin, Z., Gao, Y., Trafas, B. M., Weaver, J. H. *Phys. Rev. B* (1988) **38,** 10776.

17. Zhou, X. L., White, J. M. Surf. Sci., (1991) **241**, 244.

18. Ibuki, T., Hiraya, A., Shobatake, K., Matsumi, Y., Kawasaki, M. *Chem. Phys. Lett* (2) (1989) **160,** 152.

19. Bancroft, G. M., Coatsworth, L. L., Creben, D. K., Tse, J. *Phys. Scr.* (5-6) (1977) **16**, 217.

20. Maslowsky, E. *Vibrational Spectra of Organometalic Compounds*; John Wiley and Sons, Inc., 1977.

21. Froitzheim, H., Kohler, M., Lammering, H. *Phys. Rev.B* (1984) **30,** 5771.

Figure Captions

Figure 1. Schematic diagram of the apparatus used in this work.

Figure 2. UPS spectra of clean Si(110) and TMIn dosed (0.5 L,300 K) Si(110) before and after annealing to the indicated temperatures.

Figure 3. C 1s XPS spectra taken from TMIn dosed (5 L, 300 K) Si(110) before and after annealing to the indicated temperatures.

Figure 4. In $3d_{3/2,5/2}$ XPS difference spectra taken from TMIn dosed (150 L, various T) Si substrates after dosing at the indicated temperatures (pre-anneal) and after annealing the dosed sample to 1000 K (post-anneal).

Figure 5. HREELS spectra of TMIn(ad) (0.5 L, 140 K)/Si (110) and after subsequent annealing to the indicated temperatures.

UHV Gas-Surface Reaction System with Multiple Diagnostics

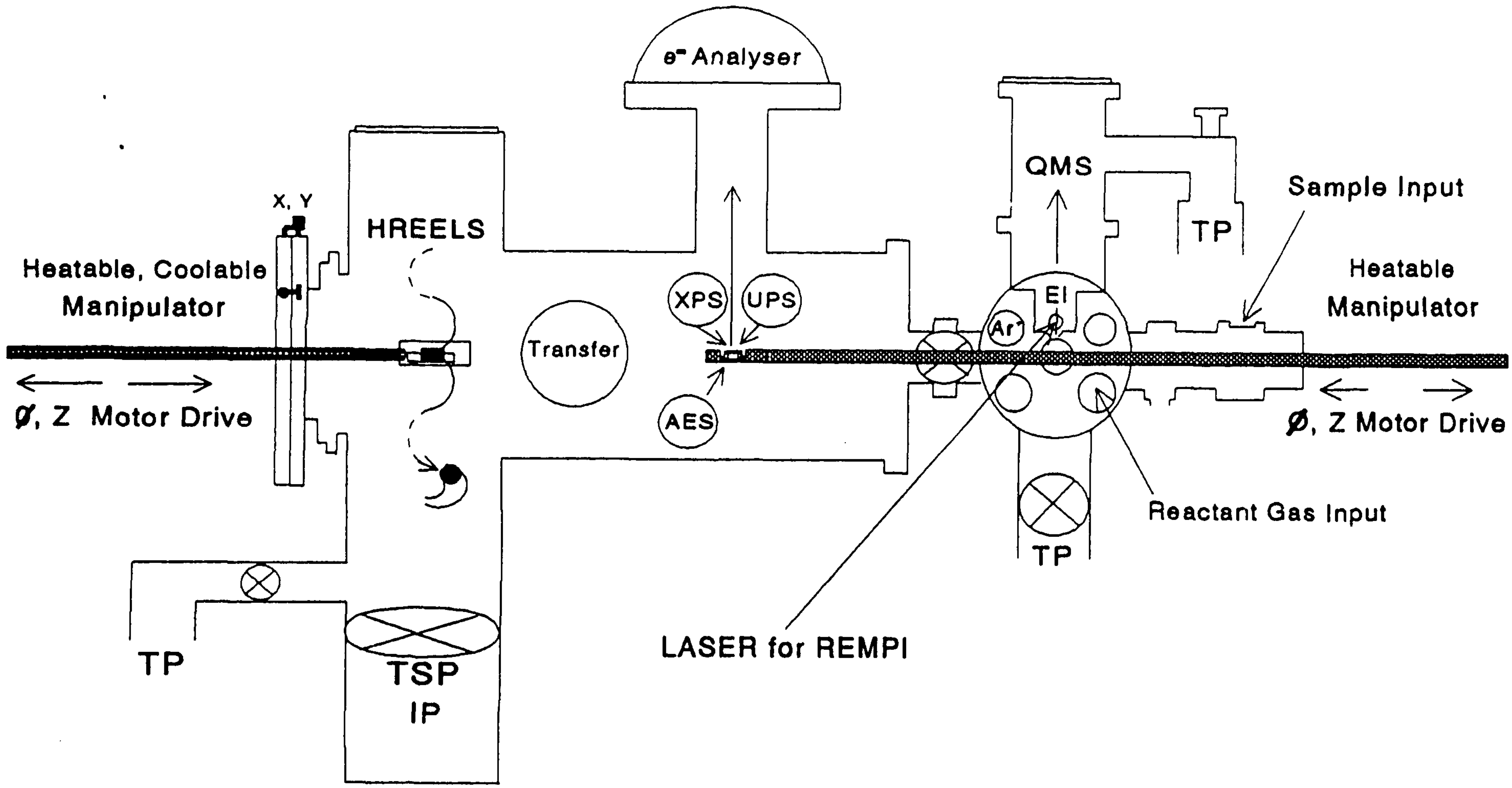

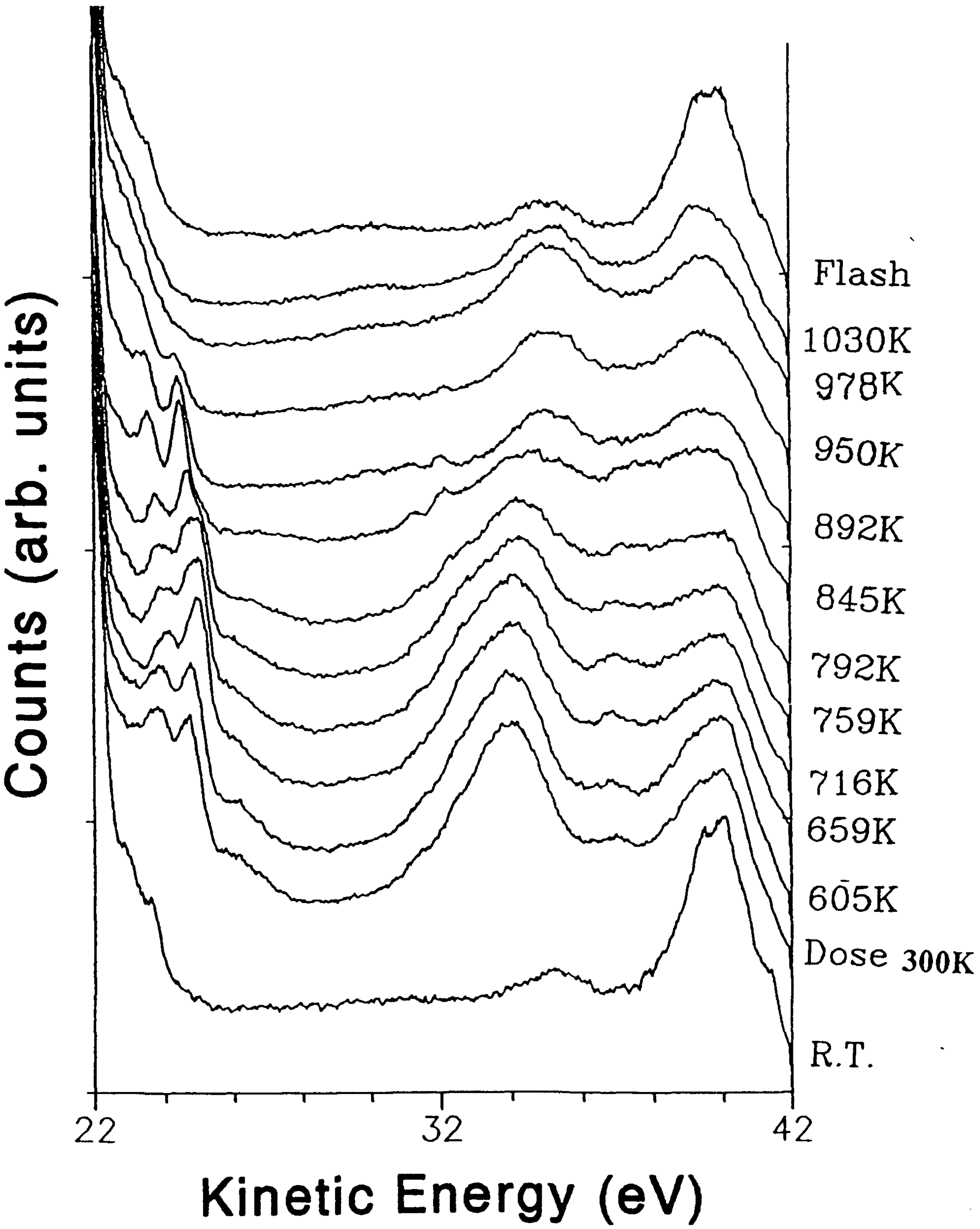
Counts (arb. units)
Flash
1030K
978K
950K
892K
845K
792K
759K
716K
659K
605K
Dose 300K
R.T.
22
32
42
Kinetic Energy (eV)

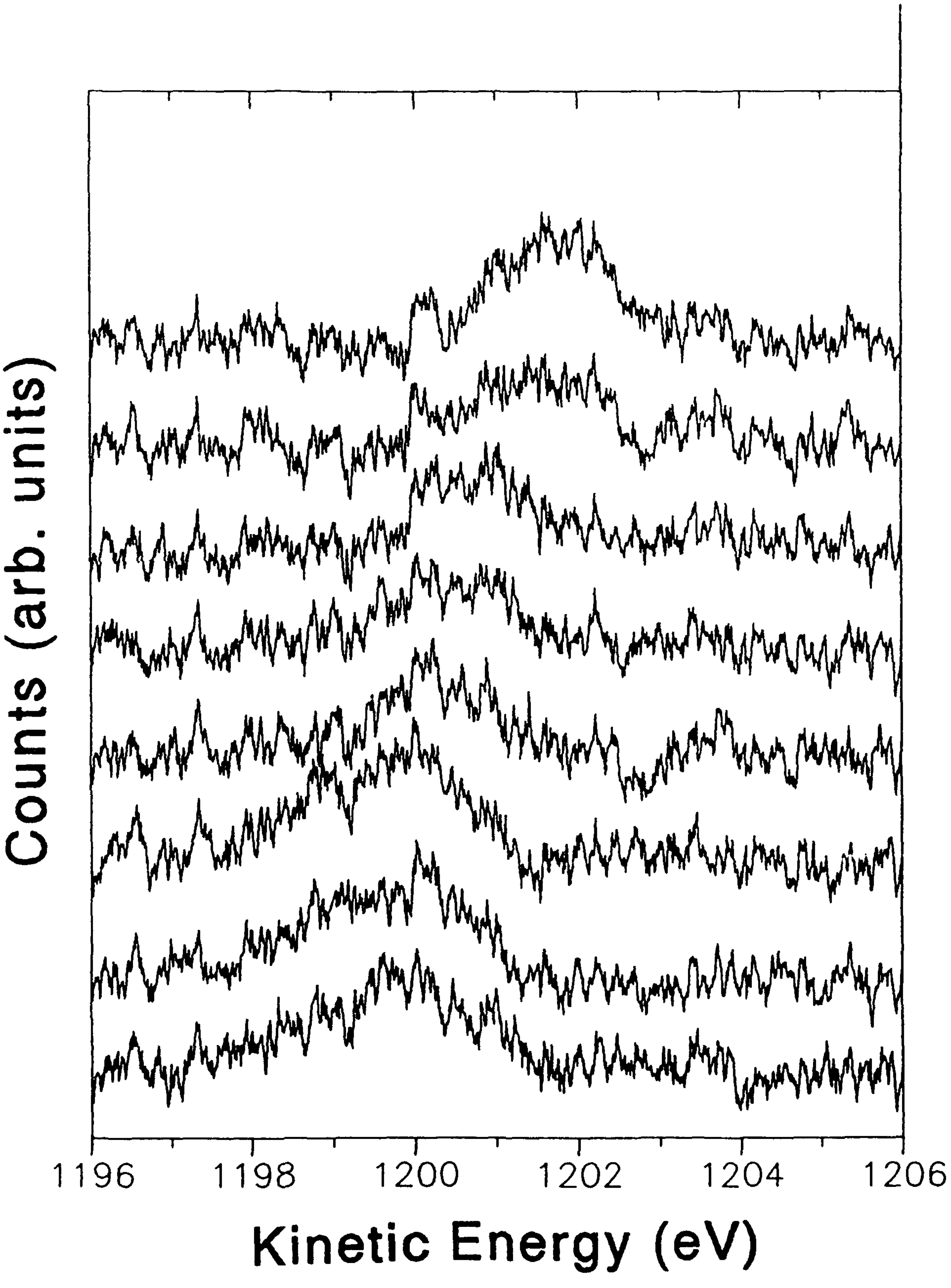
Counts (arb. units)
1196
1198
1200
1202
1204
1206
Kinetic Energy (eV)

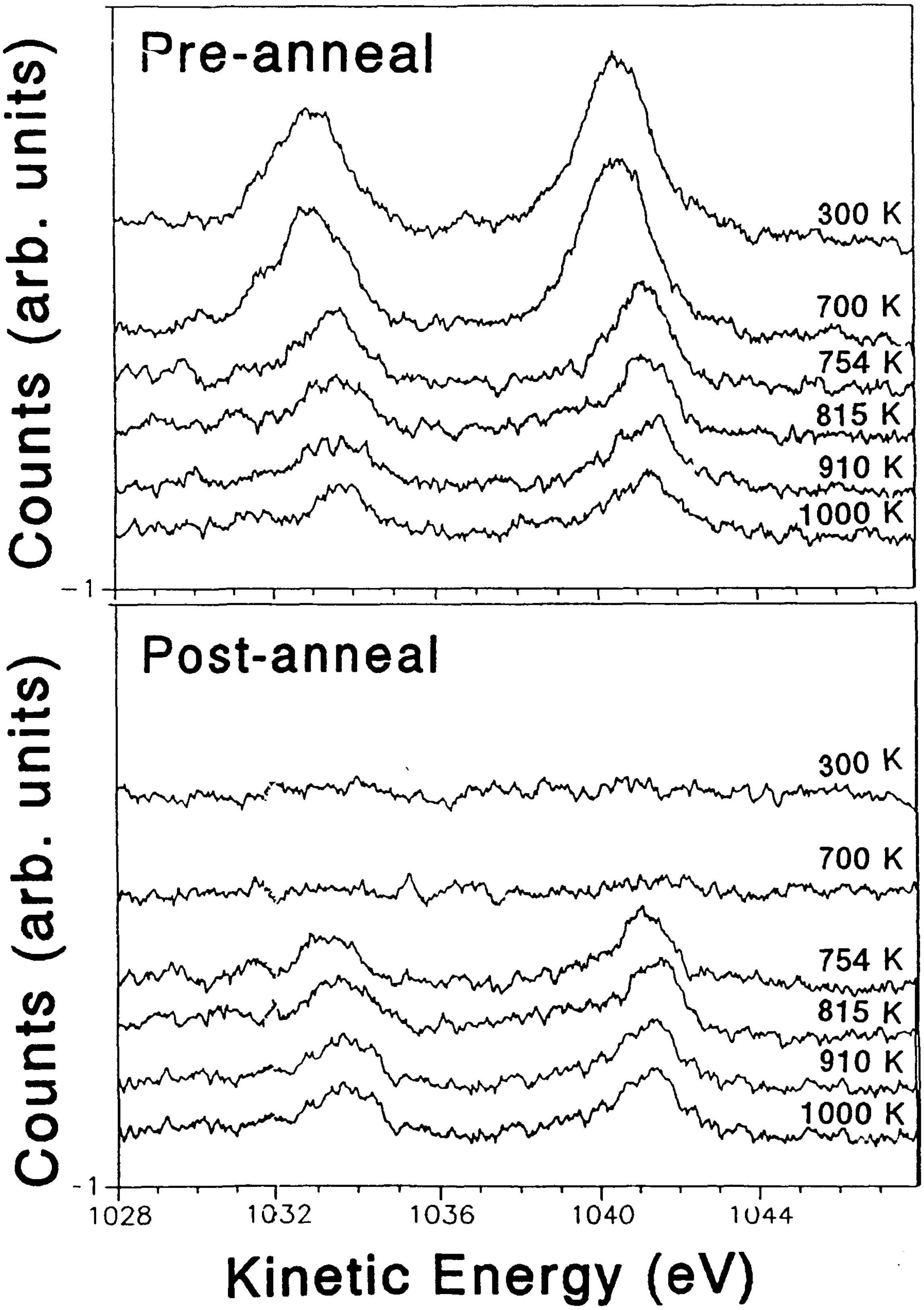
Pre-anneal
Post-anneal
Counts (arb. units)
Counts (arb. units)
300 K
700 K
754 K
815 K
910 K
1000 K
300 K
700 K
754 K
815 K
910 K
1000 K
-1
-1
1028
1032
1036
1040
1044
Kinetic Energy (eV)

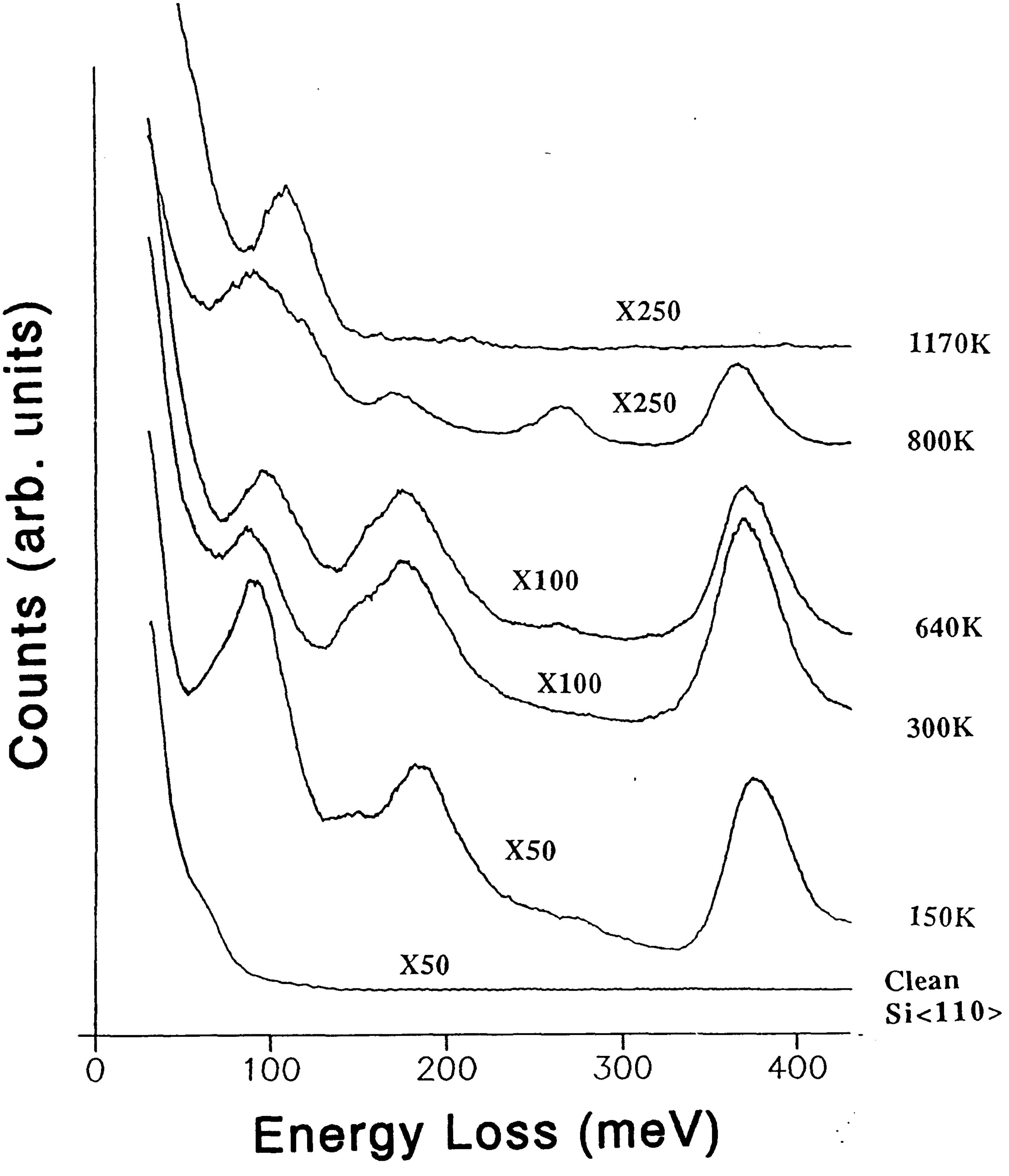
Counts (arb. units)
X250
1170K
X250
800K
X100
640K
X100
300K
X50
150K
X50
Clean
Si<110>
0
100
200
300
400
Energy Loss (meV)